NASA TN D-229

7N-05
198495
249

NASA TN D-229

TECHNICAL NOTE
D-229

EXPERIMENTAL INVESTIGATION OF THE EFFECT OF ASPECT RATIO AND MACH NUMBER ON THE FLUTTER OF CANTILEVER WINGS

By E. Widmayer, Jr., W. T. Lauten, Jr., and S. A. Clevenson

Langley Research Center
Langley Field, Va.

NATIONAL AERONAUTICS AND SPACE ADMINISTRATION

WASHINGTON April 1960

NATIONAL AERONAUTICS AND SPACE ADMINISTRATION

TECHNICAL NOTE D-229

EXPERIMENTAL INVESTIGATION OF THE EFFECT OF ASPECT RATIO AND MACH NUMBER ON THE FLUTTER OF CANTILEVER WINGS[1]

By E. Widmayer, Jr., W. T. Lauten, Jr., and S. A. Clevenson

SUMMARY

The results of some wind-tunnel experiments to investigate the effects of aspect ratio and Mach number on the flutter of uniform, unswept, cantilever wings are reported. Models having aspect ratios ranging from 2 to 13 were tested at Mach numbers up to 0.92. No general attempt is made to correlate the data with three-dimensional-flow theory, but an examination of the data is made on the basis of reference theoretical values obtained from the two-dimensional incompressible-flow theory. On this basis a reduction in aspect ratio, in general, increased the ratio of the experimental flutter speed to the calculated flutter speed. The analysis also indicated that for a given aspect ratio, the flutter-speed ratio decreased slightly as the Mach number was increased.

INTRODUCTION

In the problem of flutter, accurate evaluation of the effects of finiteness of span and of compressibility has been difficult. The application of a two-dimensional incompressible-flow analysis to the flutter problem of wings of large aspect ratio, in the neighborhood of 6 and above, has been sufficient, in most cases of low-speed aircraft, to yield an engineering solution. For aircraft designed for high subsonic speeds, the application of a two-dimensional incompressible-flow analysis needs some modification. Moreover, the application also required modification for low-aspect-ratio wings where the flow pattern deviates to a considerable extent from the assumption of two-dimensional flow.

The subject of aspect-ratio effects on flutter has been dealt with theoretically by the application of theoretical air forces for three-dimensional flow on an oscillating wing. Despite the many theoretical investigations of these air forces (refs. 1 to 10), the theory is still

---

[1]Supersedes declassified NACA RM L50C15a, by E. Widmayer, Jr., W. T. Lauten, Jr., and S. A. Clevenson.

incomplete, even for the incompressible case. This incompleteness is due partly to the difficulty of mathematically representing the physical phenomena and partly to the approximations necessary to obtain a solution. Certain of these approximations are in doubt, particularly those associated with tip effects. Reference 11 proposes a method to account better for the physical phenomena in the region of the tip. These various methods are difficult and laborious to apply numerically and consequently their practical application to flutter has been limited.

With regard to experimental work, insufficient data are available on the effects of aspect ratio and of compressibility on the flutter of wings. This lack of data is due in part to difficulties in experimental technique and in part to difficulties in isolating the various effects. In order to supply additional data on these effects, a series of tests has been conducted to furnish information on the subject, and the results are reported herein. Cantilever wings having aerodynamic aspect ratios varying from 2 to 13 and models with end plates to simulate infinite aspect ratios were employed. The experiments included a range of Mach numbers up to 0.92. No attempt is made to correlate the data with the various three-dimensional theories. However, it is convenient and useful to employ two-dimensional incompressible-flow theory (ref. 12) to establish reference values to serve as a basis for comparison and discussion of the results.

SYMBOLS

b — wing semichord, ft

c — wing chord, measured perpendicular to leading edge, in.

l — wing length, measured along leading edge, in.

m — mass of wing, slugs/ft

A_g — geometric aspect ratio, l/c

A — aerodynamic aspect ratio, $2A_g$

M_{cr} — theoretical Mach number at which sonic velocity is first attained over wing section at zero lift

x_o — distance of elastic axis from leading edge, percent chord

x_1 — distance of center of gravity from leading edge, percent chord

a — nondimensional elastic axis position, $\frac{2x_o}{100} - 1$

$a + x_\alpha$ nondimensional center-of-gravity position, $\frac{2x_1}{100} - 1$

r_α nondimensional radius of gyration of wing about elastic axis

g_α structural damping coefficient in torsion

g_{h_1} structural damping coefficient in first bending

GJ torsional stiffness, lb-in.^{2}

EI bending stiffness, lb-in.^{2}

f_{h_1} first bending natural frequency, cps

f_{h_2} second bending natural frequency, cps

f_t first torsion natural frequency, cps

f_α first torsion natural frequency relative to elastic axis, cps

f_e experimental flutter frequency, cps

f_R reference flutter frequency, cps

ρ density of testing medium at time of flutter, slugs/cu ft

q dynamic pressure at flutter, lb/sq ft

V_e experimental flutter speed, mph

V_R reference flutter speed, mph

M Mach number at flutter

κ wing mass-density ratio at flutter, $\pi\rho b^2/m$

MODELS

In order to obtain a desired range of flutter speeds, different types of construction were used for the models; some models were made of solid spruce, some were made of balsa wood with various aluminum-alloy inserts, and some were made of rib-and-fabric construction. The model cross sections and dimensions are shown in figures 1 to 6. In determining the aerodynamic aspect ratio, referred to herein as aspect ratio, the tunnel wall is considered to act as a reflecting surface and the aspect ratio is assumed to be twice the geometric aspect ratio. Models incorporating a range of aspect ratios (13, 12, 9, 7, 6, 4, and 2) were investigated and their pertinent geometric structural properties are given in table I. The number preceding the dash in the model designations indicates the aspect ratio.

Models 12-1, 12-2, 9-1, 9-2, 6-1, and 6-2 were of balsa and aluminum-alloy plate construction. Models 12-1 and 12-2 ($A = 12$) were later cut down to aspect ratio 9 to make models 9-1 and 9-2, respectively. Further cutting to $A = 6$ produced models 6-1 and 6-2. The cross sections of these models are shown in figure 1.

L
8
1
7

Sketches of the large aspect-ratio models (12-3 to 12-7) showing their airfoil sections and construction are given in figure 2. These models had 8-inch chords and 48-inch lengths (aspect ratio 12) and the same general structural design as models 12-1 and 12-2. Model 13-1, which had a chord of 4 inches and a length of 26 inches (aspect ratio 13), had an unconventional section for which the ordinates are given in figure 3.

The aspect-ratio-7 models (7-1 to 7-6) shown in figure 4, consisted of spanwise balsa laminations glued to a duralumin box made from 0.016-inch sheet. The aspect-ratio-4 models (4-1 and 4-2) shown in figure 5 were of solid spruce construction. To reduce the torsional stiffness of these models, chordwise slots were cut from the trailing edge forward, perpendicular to the plane of the wing, and were spaced at intervals of 1 inch.

Figure 6 shows the details of the aspect-ratio-2 models. In order to obtain flutter at this low aspect ratio, thin sections and rib-and-fabric construction were employed. Model 2-5 was a 15° sheared swept-back wing of similar construction.

EQUIPMENT

The tests were conducted in the Langley 4.5-foot flutter research tunnel which is of the closed-throat, single-return type employing either air, Freon-12, or a mixture of air and Freon-12 as a testing medium at absolute pressures varying from 4 inches to 30 inches of mercury. In Freon-12 at standard pressure and temperature the speed of sound is 324 miles per hour and the density is 0.0106 slug per cubic foot.

The maximum choking Mach number for these tests was approximately 0.92. The Reynolds number range was from 0.434×10^6 to 5×10^6.

It may be appropriate to mention that the variation of γ, the ratio of specific heats at constant pressure and at constant volume, resulting from the use of air, Freon-12, or a mixture of air and Freon-12 is thought to have relatively minor effect on flutter as compared with the effects associated with Mach number. Theoretical considerations for a stationary airfoil in steady flow which permit the inclusion of γ (see, for example, ref. 13) tend to substantiate this, at least for the range of Mach numbers concerned. Reference 14 presents a comparison of flutter data taken in air with flutter data taken in Freon-12, which indicates no appreciable effects of the index γ of the test medium.

The models were mounted from the top of the tunnel as cantilever beams with rigid bases. Two sets of strain gages were fastened near the root of each model, one set for recording principally the bending deformations and the other set for recording principally the torsional deformations.

Models with end plates were used in the tunnel to simulate infinite aspect ratio. The end plates were made of $\frac{1}{4}$- inch steel plate with beveled edges, had 15-inch chords, and spanned the tunnel. The gap between wing tip and end plate was of the order of 0.01 to 0.02 inch. A strut was added from the midspan of the plate to the floor of the tunnel in order to minimize the deflection of the plate.

TEST PROCEDURE

During each test the tunnel speed was slowly increased until the model fluttered. At this instant, the tunnel conditions were noted and an oscillograph record of the strain gage output was taken. The tunnel speed was then immediately reduced in an effort to prevent destruction of the model. The experimental flutter speed V_e, the density of testing medium ρ, and the Mach number M were determined from the tunnel data, and the experimental flutter frequencies were determined from the oscillograms. The natural frequencies of the models in bending and torsion at zero airspeed were recorded before each test. The wing damping coefficients (ref. 15) in bending and torsion $\left(g_{h_1}\right.$ and $\left.g_{\alpha}\right)$ were obtained from the decay records of the natural frequencies.

RESULTS AND DISCUSSION

The results of the investigation are listed in detail in table II.
While the data presented do not allow a quantitative critical appraisal
of the various existing three-dimensional-flow theories, sufficient
information pertaining to test conditions is supplied to permit an engi-
neering evaluation of these theories with respect to their application
to a flutter analysis. As a basis for presenting and comparing results,
ratios of experimental flutter velocities V_e to reference flutter
velocities V_R are determined so that the data may indicate more clearly L
the effects of aspect ratio and Mach number. The reference flutter veloc- 8
ity V_R is calculated by the method of reference 12, which assumes an 1
idealized, uniform, infinite, rigid wing mounted on springs in an incom- 7
pressible medium and uses uncoupled first bending and uncoupled first
torsion frequencies. In the present work where the theory is applied to
cantilever wings, the first bending (natural) coupled frequency and the
uncoupled first torsion frequency were used. The density used was that
of the testing medium measured at the time of flutter. The calculations
also yield a corresponding reference flutter frequency f_R which is use-
ful in comparing frequency data.

It may be remarked that the test procedure employed in this work was adapted to obtaining over-all results conveniently and to obtaining reference theoretical values easily. This work, then, establishes orders of magnitude of integrated effects especially useful for engineering purposes. This procedure has the disadvantage that a more quantitative separation of the effects of aspect ratio, mode shape, and Mach number is necessary to allow refined comparisons with available theories.

The effect of the use of first bending and first torsion modal shapes in the calculation of a theoretical flutter speed was investigated by calculating flutter speeds from the theory of reference 16 for some of the wings reported. The calculated speeds were identical to those determined by reference 15. The flutter speeds obtained from these calculations involving mode shape are not presented, but were found to exceed V_R by approximately 3 percent.

The effect of higher modes on a theoretical flutter speed for two-dimensional flow could also be determined. However, the effect of aspect ratio is a function of modal shape in addition to plan form, so that a comparison of experimental values involving higher modes with those experimental values involving only first bending and first torsion modes would be misleading. For this reason, in those cases where a definite departure from the first bending and first torsion modes was indicated by observation or by recorded flutter, the data, while presented, were not considered for plots or in the analysis of the aspect ratio and compressibility effects. The higher-mode flutter is indicated in the remarks column of table II. Also indicated in the remarks are those cases where apparent flutter was noted visually but subsequent inspection of the oscillograms indicated that the wing did not flutter. The V_e in these cases is the speed at which the data were taken and does not indicate an experimental flutter speed as defined in the section entitled "Symbols." For the cases in which higher-mode flutter was observed, some comparison might be worth while in which the reference flutter speed is taken as the theoretical value which is determined when higher modes are included.

Summary plots to illustrate the significant effects of aspect ratio and Mach number on the flutter speed of the various models are presented in figures 7 and 8. For convenience in distinguishing data points in the significant ranges, the data in figure 7 for Mach numbers above 0.6 and in figure 8 for aspect ratios above 6 are shown by solid symbols.

In figure 7, graphical representation of the data is made showing the effect of aspect ratio on V_e/V_R. The data for $A = 7$ are somewhat in doubt because of the absence of precise measurements of the model parameters. The presence of the tunnel-wall boundary layer acts to reduce the effective aspect ratio on all models, the wings of lower aspect ratio being most sensitive to this factor. Since the structural requirements to obtain flutter necessitated the use of wings having various thickness ratios, the results also may be somewhat influenced by the thickness ratio. However, there is a discernible trend for the ratio V_e/V_R to increase from an asymptotic value as A is decreased. It may also be seen that for the higher values of A the reference velocity is, in most instances, close to, but less than, the experimental value of the flutter velocity.

In figure 8, V_e/V_R is plotted against Mach number. It may be noted that for a specific aspect ratio there exists a trend for the ratio V_e/V_R to decrease as the Mach number increases. In an attempt to study flutter at simulated infinite aspect ratio, an end plate was placed near the tip of an aspect-ratio-4 wing. While it is not possible to ascertain the precise effect of the gap between the wing tip and plate, it may be seen in figure 8 that the end plate decreases the value of the ratio V_e/V_R as compared with the values obtained without an end plate, as well as decreasing the value below that obtained for the aspect-ratio-12 models. A comparison of values of V_e/V_R for the aspect-ratio-4 model without an end plate to the aspect-ratio-4 model with an end plate showed a decrease in the value of the ratio of approximately 12 percent which may be attributed to the effect of aspect ratio.

CONCLUDING REMARKS

Some flutter data have been presented for cantilever wing models that illustrate some effects of aspect ratio and Mach number on flutter. The aspect ratio varied from 2 to 13 and the range of Mach number extended from 0.2 to 0.92.

No general attempt is made to correlate the data with theory; however, a comparison is made with a theory that assumes a two-dimensional incompressible flow. On the basis of this comparison, analysis of the data indicated that a reduction in aspect ratio, in general, increased the ratio of the experimental flutter speed to calculated flutter speed. The comparison also indicated that for a given aspect ratio, this ratio decreases slightly as the Mach number is increased.

L
8
1
7

Langley Research Center,
National Aeronautics and Space Administration,
Langley Field, Va., March 15, 1950.

REFERENCES

1. Cicala, P.: Comparison of Theory With Experiment in the Phenomenon of Wing Flutter. NACA TM 887, 1939.

2. Dingel, [M.], and Kuessner, [H. G.]: Contributions to Nonstationary Wing Theory. VIII - The Vibrating Wing of Large Aspect Ratio. Translation No. F-TS-935-RE, Air Materiel Command, U.S. Army Air Force, May 1947.

3. Possio, Camillo: On the Problem of the Discontinuous Motion of a Wing. Note 2. Finite Wing. Reprint from: L'Aerotecnica, vol. XXI, fasc. 3, March 1941, pp. 205-230.

4. Jones, Robert T.: The Unsteady Lift of a Wing of Finite Aspect Ratio. NACA Rep. 681, 1940.

5. Jones, W. Prichard: Theoretical Determination of the Pressure Distribution of a Finite Wing in Steady Motion. R. & M. 2145, British A.R.C., 1943.

6. Reissner, Eric: Effect of Finite Span on the Airload Distributions for Oscillating Wings. I - Aerodynamic Theory of Oscillating Wings of Finite Span. NACA TN 1194, 1947.

7. Reissner, Eric, and Stevens, John E.: Effect of Finite Span on the Airload Distributions for Oscillating Wings. II - Methods of Calculation and Examples of Application. NACA TN 1195, 1947.

8. Biot, M. A., and Boehnlein, C. T.: Aerodynamic Theory of the Oscillating Wing of Finite Span. GALCIT Rep. No. 5, Sept. 1942.

9. Bratt, J. B., and Wight, K. C.: The Effect of Mean Incidence, Amplitude of Oscillation, Profile, and Aspect Ratio on Pitching Moment Derivatives. R. & M. No. 2064, British A.R.C., 1945.

10. Wasserman, L. S.: Aspect Ratio Corrections in Flutter Calculations. MR No. MCREXA5-4595-8-5, Air Materiel Command, Eng. Div., U.S. Air Force, Aug. 26, 1948.

11. Zartarian, Garabed, Fotieo, George, and Ashley, Holt: Theoretical and Experimental Methods of Flutter Analysis. Phase 8 - Analysis of Tip Effects on the Aerodynamic Forces on an Oscillating Wing. Contract No. NOa(s)8790, vol. VII, M.I.T. Rep., Bur. Aero., June 30, 1949.

12. Theodorsen, Theodore, and Garrick, I. E.: Mechanism of Flutter - A Theoretical and Experimental Investigation of the Flutter Problem. NACA Rep. 685, 1940.

13. Kaplan, Carl: Effect of Compressibility at High Subsonic Velocities on the Lifting Force Acting on an Elliptic Cylinder. NACA Rep. 834, 1946. (Formerly NACA TN 1118.)

14. Castile, George E., and Herr, Robert W.: Some Effects of Density and Mach Number on the Flutter Speed of Two Uniform Wings. NACA TN 1989, 1949.

15. Smilg, Benjamin, and Wasserman, Lee S: Application of Three-Dimensional Flutter Theory to Aircraft Structures. ACTR No. 4798, Materiel Div., Army Air Corps, July 9, 1942.

16. Barmby, J. G., Cunningham, H. J., and Garrick, I. E.: Study of Effects of Sweep on the Flutter of Cantilever Wings. NACA Rep. 1014, 1951. (Supersedes NACA TN 2121.)

L
8
1
7

TABLE I.- GEOMETRIC AND STRUCTURAL PROPERTIES OF MODELS

Model	A_g	A	NACA airfoil section	M_{cr}	b, ft	x_o, percent chord	x_1, percent chord	a	$a + x_\alpha$	r_α^2	g_α	g_{h_1}	GJ, lb-in.^{2}	EI, lb-in.^{2}
12-1	6	12	16-010	0.79	0.333	45.8	49.6	-0.084	-0.008	0.21	0.0153	0.0210	48,000	45,570
12-2	6	12	16-010	.79	.333	48.0	49.0	-.040	-.020	.163	.0258	.0460	36,500	135,500
12-3	6	12	65-010	.75	.333	31.25	45.1	-.375	-.098	.240	.0204	.0263	130,000	99,150
12-4	6	12	0010	.75	.333	34.4	46.2	-.312	-.076	.221	.0131	.0195	97,000	112,400
12-5	6	12	16-016	.74	.333	48.3	43.7	-.034	-.126	.201	.0231	.0405	75,500	369,800
12-6	6	12	16-006	.87	.333	47.5	50.0	-.050	-.000	.125	.0291	.0050	34,880	38,600
12-7	6	12	16-010	.79	.333	43.8	46.6	-.124	-.068	.178	.0185	.0312	41,200	18,300
13-1	6.5	13	(a)	.66	.167	14.1	46.6	-.719	-.068	.629	.0576	(b)	10,850	120,200
9-1	4.5	9	16-010	.79	.333	48.1	49.6	-.038	-.008	.21	.0130	.0257	48,000	45,570
9-2	4.5	9	16-010	.79	.333	48.0	49.0	-.040	-.020	.163	.0222	.0183	36,500	135,500
9-3	4.5	9	16-010	.79	.333	48.4	49.0	-.032	-.020	.160	.0183	.0101	28,440	83,700
7-1	3.5	7	16-010	.79	.167	36.0	46.2	-.280	-.076	.301	.0379	.0163	(b)	(b)
7-2	3.5	7	16-010	.79	.167	37.0	46.2	-.260	-.076	.292	.0587	.0338	2,580	9,900
7-3	3.5	7	16-010	.79	.167	40.0	47.0	-.200	-.060	.280	.0485	.0257	(b)	(b)
7-4	3.5	7	16-010	.79	.167	43.8	46.9	-.124	-.062	.293	.0371	.0238	3,000	(b)
7-5	3.5	7	16-010	.79	.167	40.6	47.7	-.188	-.046	.310	.0442	.0228	3,390	5,120
7-6	3.5	7	16-010	.79	.167	41.2	47.5	-.176	-.050	.304	(b)	(b)	(b)	(b)
6-1	3	6	16-010	.79	.333	48.5	49.6	-.030	-.008	.210	.0129	.0247	48,000	45,570
6-2	3	6	16-010	.79	.333	43.5	49.0	-.130	-.020	.163	.0204	.0167	36,500	135,500
4-1	2	4	16-005	.87	.333	31.3	49.2	-.374	-.016	.380	(b)	(b)	3,529	26,750
4-2	2	4	16-005	.87	.333	31.3	49.2	-.374	-.016	.380	.0221	.0258	5,410	23,000
2-1	1	2	16-005	.87	.333	29.7	46.8	-.406	-.064	.347	.0577	.0450	(b)	(b)
2-2	1	2	16-005	.87	.333	33.5	46.8	-.330	-.064	.310	.0540	.0178	4,250	3,190
2-3	1	2	16-005	.87	.333	31.2	47.7	-.376	-.046	.340	.0355	.0215	1,810	4,080
2-4	1	2	16-005	.87	.333	29.0	46.0	-.420	-.080	.345	.0381	.0230	5,150	2,910
[c]2-5	1	2	16-005	.87	.333	38.8	47.2	-.224	-.056	.268	.0489	.0153	4,760	3,120

[a]See figure 3 for coordinates.
[b]Not available.
[c]15° sweepback.

TABLE II.- EXPERIMENTAL RESULTS OF INVESTIGATION

Model	f_{h_1}, cps	f_{h_2}, cps	f_t, cps	f_α, cps	f_e, cps	f_R, cps	ρ, slugs/cu ft	q, lb/sq ft	V_e, mph	V_R, mph	$\frac{V_e}{V_R}$	M	$\frac{1}{\kappa}$	Remarks
12-1	3.9	(a)	34.1	33.5	16	15.0	0.00234	67.0	165	153.5	1.075	0.216	50.3	
12-2	5.4	(a)	39.7	39.7	14.2	14.6	.00060	70.8	329	287	1.146	.429	156.5	
	5.4		39.7	39.7	14.6	15.5	.00110	71.3	245	214	1.146	.313	85.6	
	5.4	(a)	39.7	39.7	16.1	16.9	.00224	78.1	179	153	1.166	.233	42.1	
12-3	4	25.2	52	42.9	(b)	24.1	.00817	193.0	[c]148	147	1.006	.433	19.5	No flutter - second bending
12-4	4.1	27.0	53.5	46.3	28.9	20.3	.00836	197	146	161	.907	.440	19.4	Possible second bending mode
	4.1	27.0	53.3	46.1	29.8	23.6	.00226	167	262	311	.843	.346	71.7	Possible second bending mode
	4.1	27.0	53.6	46.4	27.9	19.2	.00096	87	289	434	.666	.786	169.3	Possible second bending mode
12-5	7.5	54.3	48.9	47.8	41.8	24.4	.00112	84.3	261	392	.656	.767	103.7	Possible second bending mode
	7.5	54.3	48.9	47.8	16.4	26.2	.00184	128	248	320	.776	.745	63.2	Possible second bending mode
	7.5	54.3	48.9	47.8	48.4	28.2	.00322	148	204	212	.962	.603	36.1	Possible second bending mode
12-6	3.2	19	46	45.5	18.5	13.1	.00077	59	267	267.8	.997	.689	133.3	Possible second bending mode
12-7	5.5	(a)	43	42.6	(d)	15.9	.00037	81.8	453	440	1.042	.704	273	
	4.9	(a)	41	40.6	(d)	16.1	.00040	90.0	456	433	1.053	.756	250	
	4.9	(a)	41	40.6	14.9	16.4	.00048	88.4	405	417	.971	.650	209.5	
	5.5	(a)	43	42.6	14	16.7	.00054	96.6	408	395	1.033	.536	185	
13-1	11	64	118	69.6	74	60.5	.00877	142.2	121	145	.835	.349	10.1	Possible second bending mode
	10.5	62.5	112	66	73.3	47.5	.00418	120.4	163	172	.948	.467	21.1	Possible second bending mode
	10.5	62.5	112	66	73.3	48.3	.00259	115.2	203	235.2	.863	.565	34.2	Possible second bending mode
	10.5	62.5	112	66	72	41.9	.00102	77.2	259.5	363.1	.715	.730	86.4	Possible second bending mode
	10.6	63.0	111	65.5	68	39.6	.00078	61.4	272.5	416.7	.654	.763	114	Possible second bending mode
	10.4	62.5	104	61.4	65.7	44	.00221	106.7	212	234.5	.904	.273	40	Possible second bending mode
	10.3	(a)	103	60.7	66	39.9	.00129	96.4	264	296.8	.889	.338	68.8	Possible second bending mode
	10.3	(a)	102	60.2	67	37.5	.00091	92.7	308	345.8	.89	.404	97.8	Possible second bending mode
	(d)	(a)	101	59.5	67	36.2	.00056	81.1	366.5	371	.988	.478	159.2	Possible second bending mode
	11	(a)	98	57.8	66.7	41.8	.00224	97.5	201.9	217.7	.927	.262	39.6	Possible second bending mode
9-1	7.4	(a)	44.8	44.8	25	20.8	.00227	123.3	226	211	1.071	.296	51.9	
9-2	9.53	(a)	55.7	55.7	(d)	21.1	.00057	130.4	459	406.5	1.130	.599	165.1	
	9.43	(a)	55.7	55.7	12.7	22.5	.00140	108.5	289	294	.983	.800	83.0	
9-3	8.4	(a)	52.0	52.0	(a)	20.3	.00087	74.8	282	319	.873	.776	115.4	Did not flutter
	8.4	(a)	50.5	50.5	25.3	25.8	.00903	152.1	123.9	107	1.225	.379	11.08	
7-1	40.3	(a)	149	137.7	(a)	80.4	.00212	229	[c]320	346	.925	.918	43.2	Model slotted $1\frac{1}{2}$ in. No flutter
	40.3	(a)	149	137.7	(a)	82.1	.00250	283.5	[c]322	314.5	1.025	.919	35.45	Flutter doubtful
	40.0	(a)	146	135.0	80.2	88.5	.00714	283.5	[c]190	197	.965	.553	12.82	Flutter doubtful
	40.3	(a)	149	137.7	(a)	81.2	.00236	259.5	[c]322	328	.982	.919	38.8	No flutter
	40.3	(a)	149	137.7	(a)	80.8	.00226	248	[c]322	335	.961	.918	40.5	No flutter
	40.3	(a)	149	137.7	(a)	81.8	.00255	225	[c]285	316	.902	.817	35.85	Flutter doubtful

[a]Not obtained.
[b]Data undiscernible.
[c]Speed at which data were taken.
[d]Data not available.

TABLE II.- EXPERIMENTAL RESULTS OF INVESTIGATION - CONCLUDED

Model	f_{h_1}, cps	f_{h_2}, cps	f_t, cps	f_α, cps	f_e, cps	f_F, cps	ρ, slugs/cu ft	q, lb/sq ft	V_e, mph	V_R, mph	$\frac{V_e}{V_R}$	M	$\frac{1}{\kappa}$	Remarks
7-2	36.9	(a)	139.6	128.2	52.6	76.2	0.00249	215.0	276.5	295	0.938	0.804	36.7	$1\frac{1}{2}$- in. slots
	36.9	(a)	141.0	129.3	71.0	79.1	.00308	227.0	258.5	267	.968	.746	29.7	
	34.4	(a)	137.0	125.5	68.5	78.2	.00370	226.0	236.5	239	.990	.689	24.7	
	36.4	(a)	135.4	124.0	70.4	82.1	.00774	254.0	172.4	173	.997	.498	11.85	
	(a)	(a)	(a)	(a)	(a)	76.0	.00249	271.5	[c]324.0	293	1.106	.920	36.70	No flutter
7-3	37.5	(a)	133	128.3	70.0	76.0	.00268	236.0	285.5	278	1.034	.813	34.2	$1\frac{1}{2}$- in. slots
	37.5	(a)	133	128.3	85.7	78.3	.00361	256.0	253.0	239	1.057	.734	25.3	
	37.5	(a)	133	128.3	(a)	75.8	.00259	284.0	[c]321.0	277.5	1.156	.920	35.3	No flutter
7-4	30.9	(a)	130	130	60.7	71.3	.00243	184.9	278.7	254	1.095	.355	34.8	End plate - $1\frac{1}{2}$- in. slots
7-5	32.5	(a)	127.5	123.3	70.0	74.0	.00216	199.3	292.7	292.0	1.002	.383	33.0	$1\frac{1}{2}$- in. slots
7-6	29.4	(a)	123.1	120.0	(a)	69.4	.00192	133.6	[c]252.7	280	.903	.718	37.5	End plate - $1\frac{1}{2}$ -in. slots Flutter doubtful
6-1	11.0	(a)	67.8	67.8	33.0	30.95	.00210	298	350	329.2	1.064	.475	56.1	
6-2	20.7	(a)	87.3	86.6	38.5	47.38	.00761	372	217	188	1.152	.623	12.4	
4-1	27.8	161	66.6	53.1	45.4	47.4	.00787	69.5	90.3	93.8	.986	.258	5.72	End plate - $4\frac{3}{4}$ -in. slots
4-2	28.8	159	64.0	51.1	44.8	40.9	.00215	91.9	199.6	177.0	1.108	.254	20.62	$4\frac{3}{4}$ -in. slots.
	28.6	159	63.6	50.7	35.7	38.9	.00095	50.8	222.9	243	.918	.596	44.6	End plate - $4\frac{3}{4}$ - in. slots
	28.5	159	64.2	51.2	34.4	41.1	.00225	70.3	170.6	173.5	.984	.219	19.65	End plate - $4\frac{3}{4}$ -in. slots
2-1	32.1	167	85.8	69.4	(a)	52.1	.00640	552	[c]281.5	219.7	1.28	.823	14.88	No flutter
	25.3	(a)	67.5	55.0	(d)	41.5	.00784	339	218.0	162.9	1.338	.648	12.80	
2-2	29.5	147	77.0	67.8	38.8	51.3	.00580	470	271.2	198.0	1.37	.790	16.4	
	29.5	149	77.0	67.8	39.7	51.4	.00666	468	253.0	191.5	1.31	.731	14.3	
2-3	31.9	(a)	72.6	59.7	39.8	49.7	.00398	389	292.9	212.7	1.380	.882	23.91	
	31.8	(a)	72.6	59.7	40.5	50.5	.00469	421	282.9	198.0	1.430	.864	20.23	
	33.0	(a)	75.2	61.8	43.2	53.45	.00666	467	257.4	172.0	1.495	.753	14.28	
	33.0	(a)	75.2	61.8	(a)	49.20	.00369	397	[c]321.0	229.0	1.400	.920	27.80	No flutter
2-4	24.2	155	76.5	59.8	31.8	44.62	.00380	378.2	304.7	238.8	1.277	.863	25.05	
	24.2	155	76.5	59.8	36.8	47.08	.00627	462.6	261.9	191.6	1.365	.720	15.2	
2-5	23.8	(a)	72.1	68.5	30.6	41.0	.00295	320.5	315.5	273.5	1.154	.912	35.55	15° sweep
	23.1	(a)	71.7	68.1	31.7	41.6	.00357	343.5	296.8	249.5	1.190	.874	28.80	15° sweep
	23.2	(a)	72.0	68.2	34.2	42.7	.00465	396.2	278.8	224.5	1.240	.821	22.52	15° sweep
	23.1	(a)	71.8	67.9	36.7	43.4	.00604	439.0	257.8	199.0	1.290	.760	17.35	15° sweep
	23.2	(a)	72.1	68.5	38.8	44.55	.00742	483.3	243.5	182.0	1.337	.735	14.63	15° sweep
	23.2	(a)	73.5	69.4	38.3	45.05	.00716	465.0	243.3	183.0	1.330	.718	14.12	15° sweep

[a]Not obtained.
[b]Data undiscernible.
[c]Speed at which data were taken.
[d]Data not available.

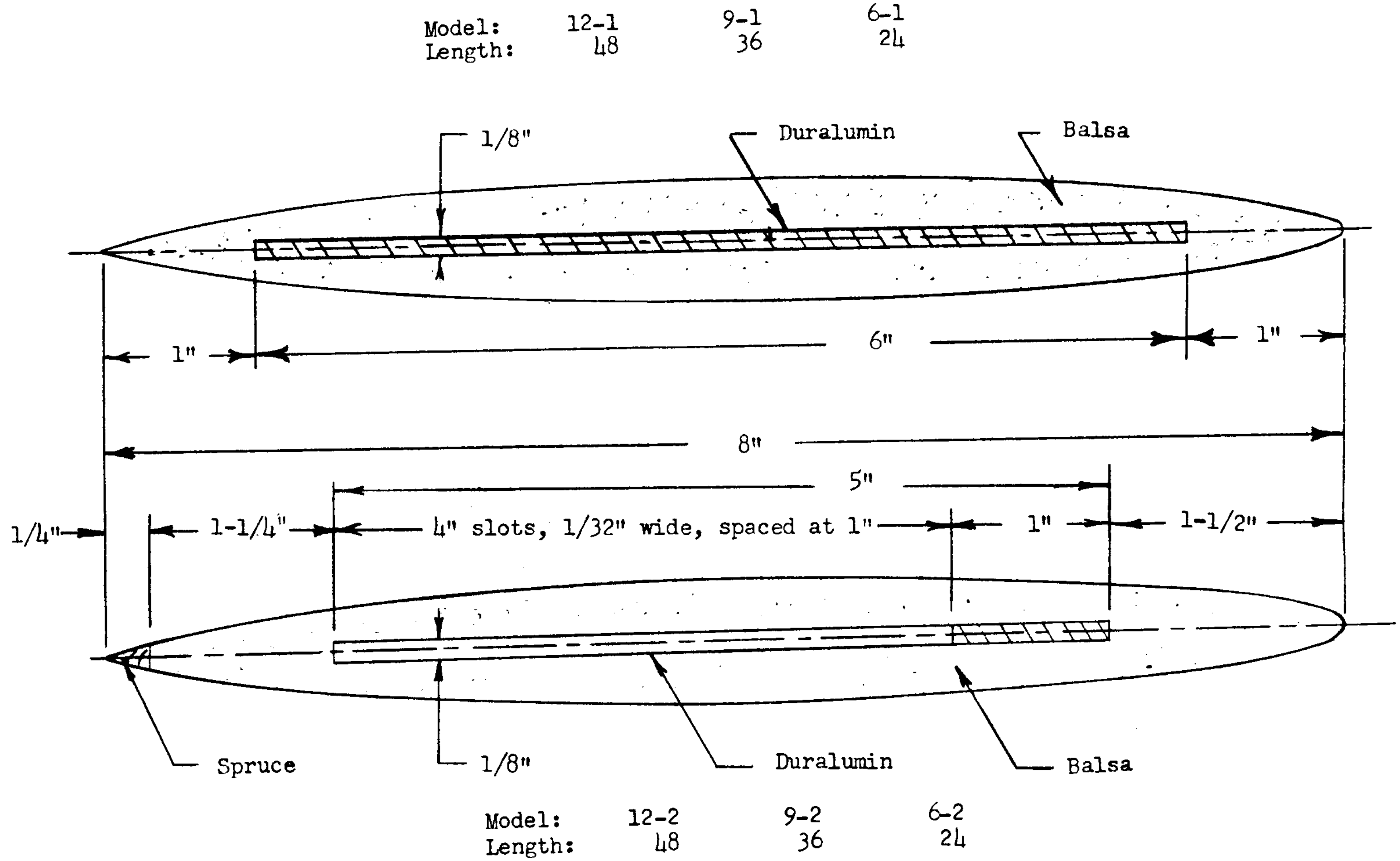

Figure 1.- Diagrams of cross sections of wing models 12-1, 9-1, 6-1, 12-2, 9-2, and 6-2.

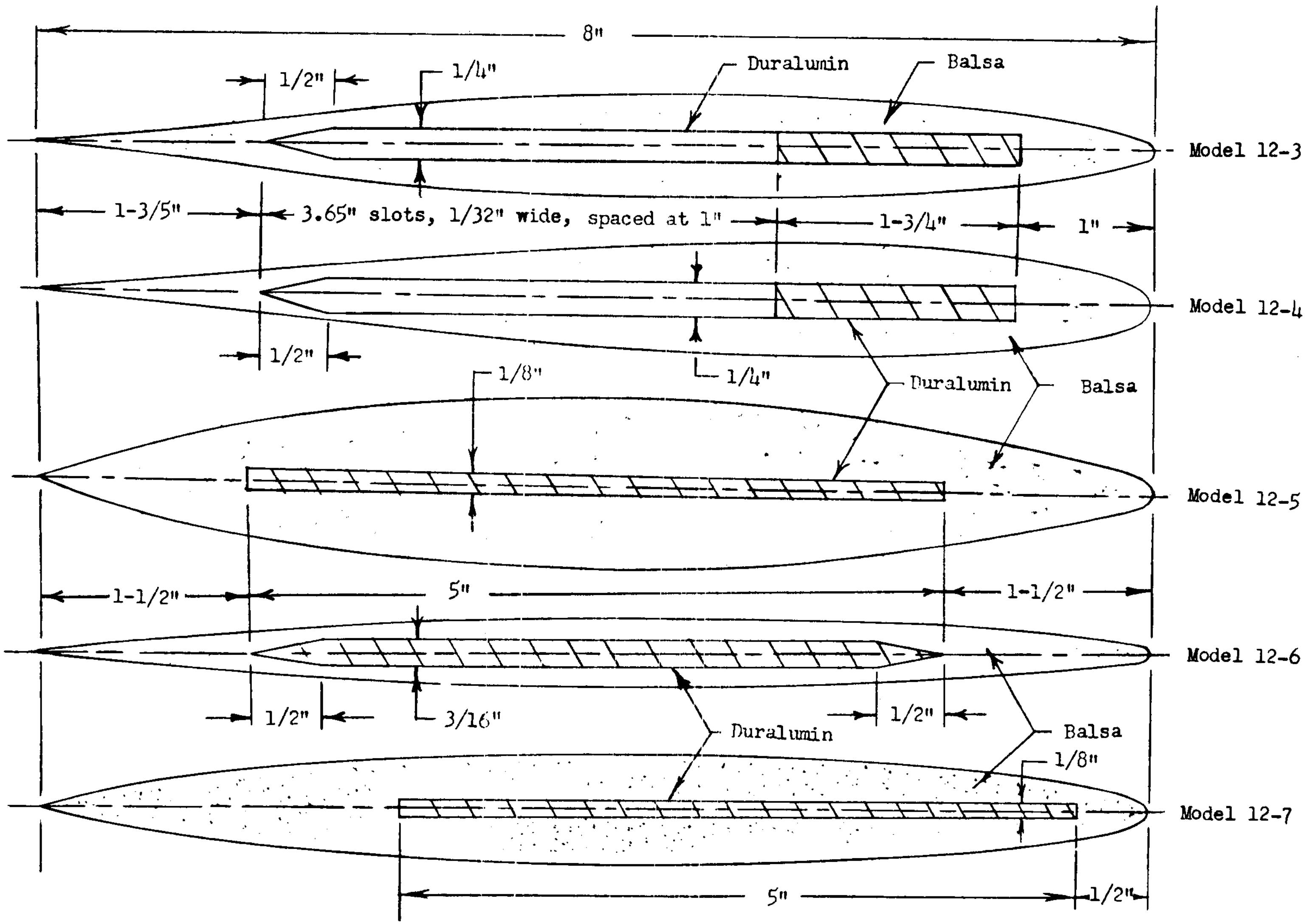

Figure 2.- Diagrams of cross sections of wing models 12-3, 12-4, 12-5, 12-6, and 12-7. A = 12.

Coordinates, percent chord	
x	$y_u = y_l$
0	0
2.5	2.92
5	4.00
10	4.95
15	4.92
20	4.55
25	4.40
37.5	3.97
50	3.55
62.5	3.05
75	2.45
87.5	1.55
92.5	1.07
97.5	.55
98.75	.42
100.00	0

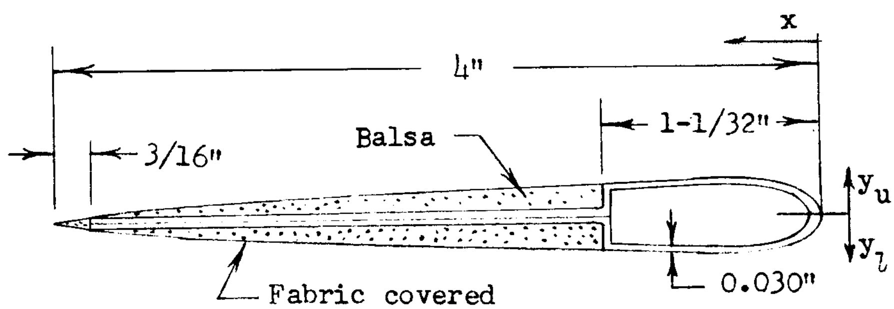

Figure 3.- Diagram of cross section and coordinates of wing model 13-1. A = 13. Wing length, 26 inches.

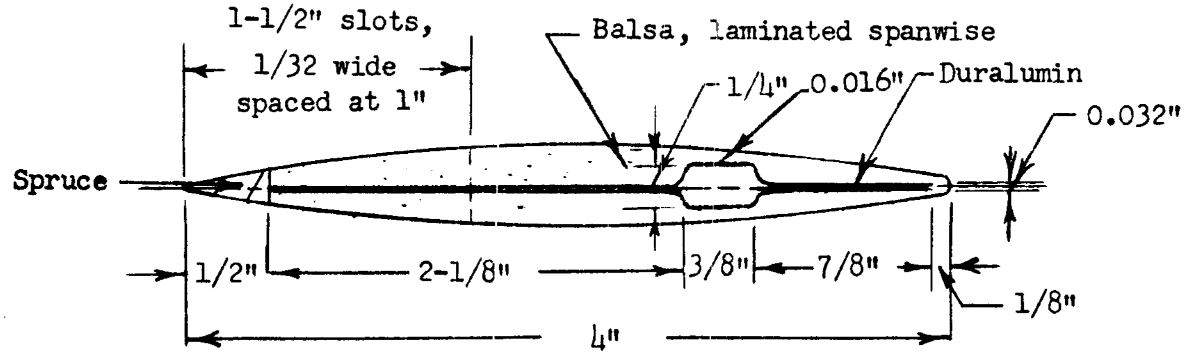

Figure 4.- Diagram of cross section of wing models 7-1 to 7-6 inclusive. A = 7.

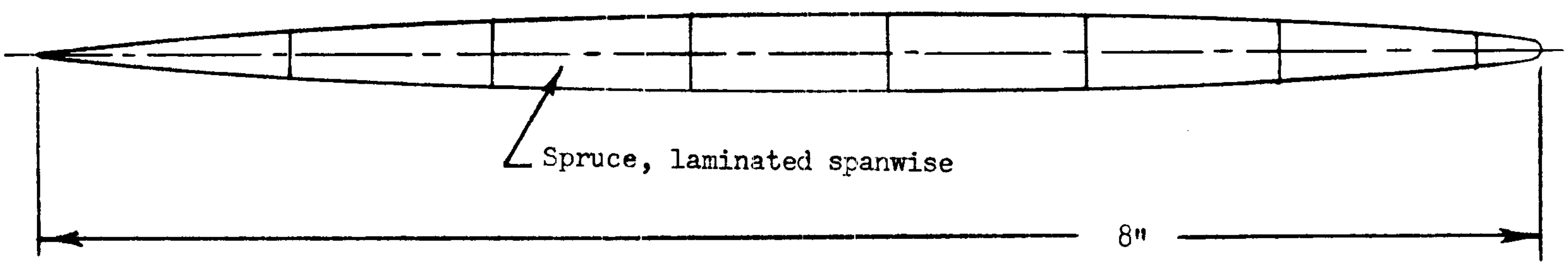

Figure 5.- Diagram of cross section of models 4-1 and 4-2. A = 4.

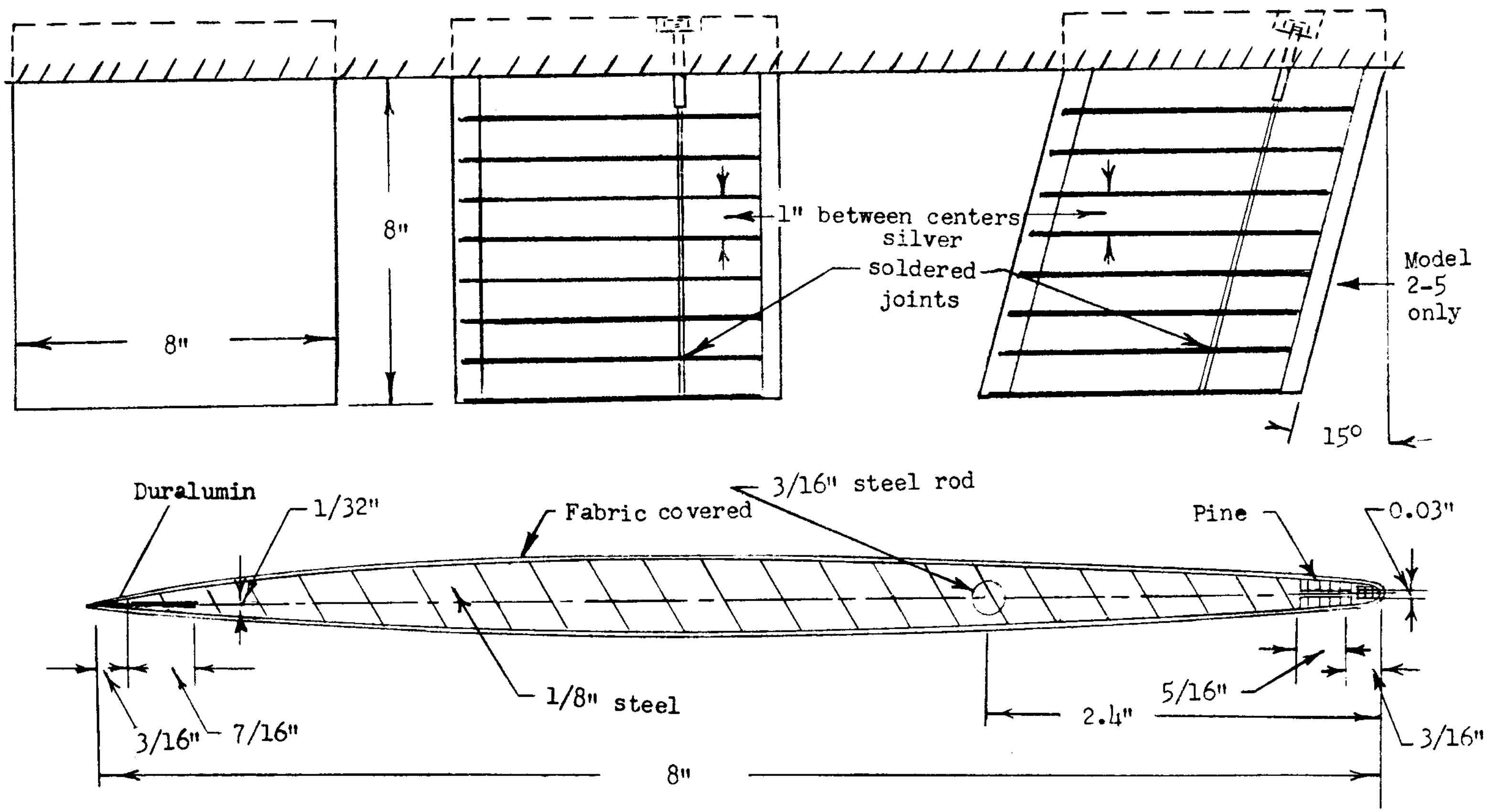

Figure 6.- Diagram of cross section and plan form of wing models 2-1 to 2-5 inclusive. A = 2.

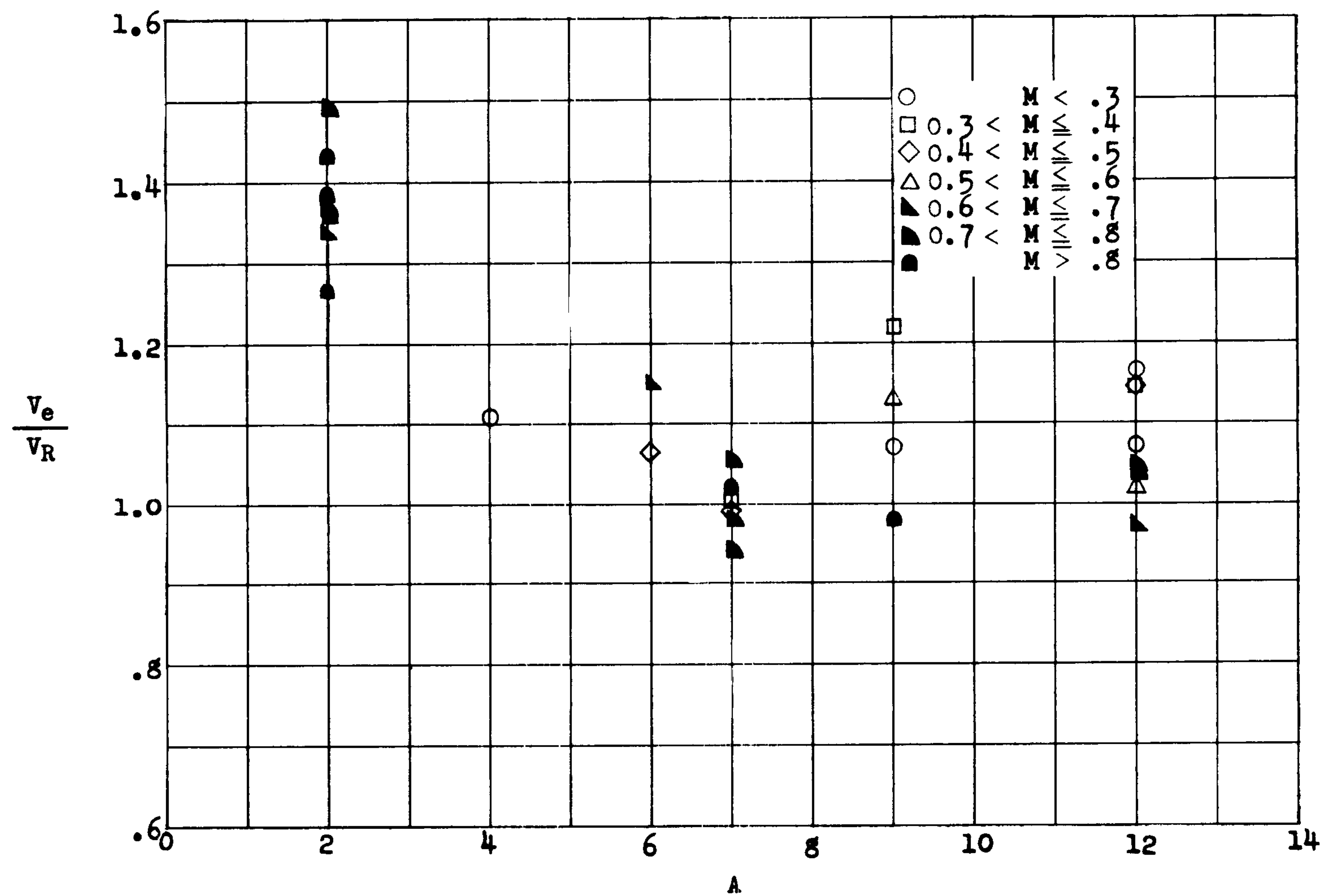

Figure 7.- Ratio of experimental flutter speed divided by reference flutter speed (V_e/V_R) against aspect ratio for various Mach numbers.

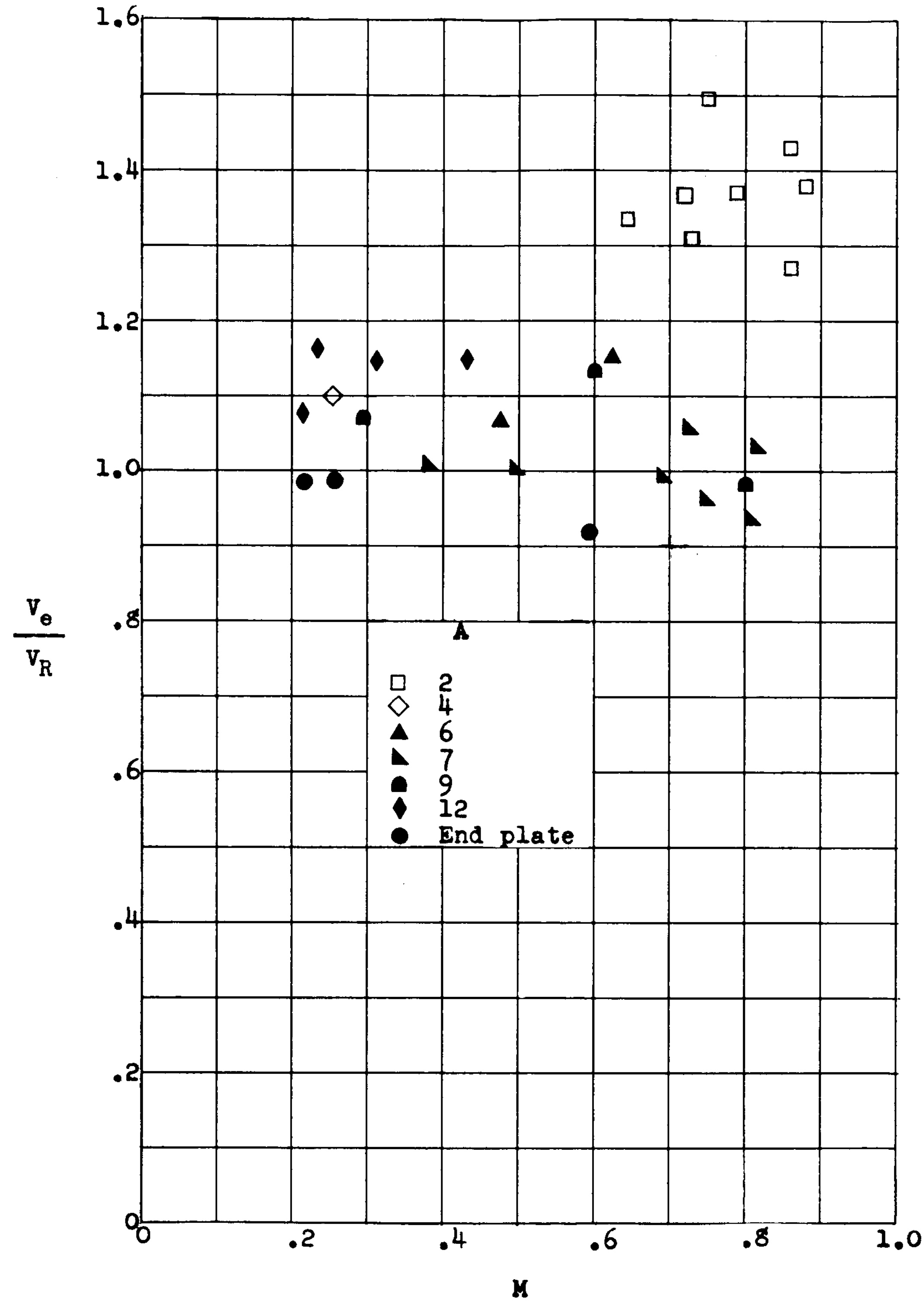

Figure 8.- Ratio of experimental flutter speed divided by reference flutter speed (V_e/V_R) against Mach number for various aspect ratios.

L-817